Available online at www.sciencedirect.com

ScienceDirect

http://www.elsevier.com/locate/biombioe

Characterization of agave bagasse as a function of ionic liquid pretreatment

Jose A. Perez-Pimienta [a,*], Monica G. Lopez-Ortega [a], Jose A. Chavez-Carvayar [b], Patanjali Varanasi [c,d], Vitalie Stavila [e], Gang Cheng [f], Seema Singh [c,d], Blake A. Simmons [c,d]

[a] Department of Chemical Engineering, Universidad Autónoma de Nayarit, Tepic, Mexico
[b] Instituto de Investigaciones en Materiales, UNAM, México D.F., Mexico
[c] Joint BioEnergy Institute, Physical Biosciences Division, Lawrence Berkeley National Laboratory, Emeryville, CA, United States
[d] Sandia National Laboratories, Biological and Materials Science Center, Livermore, CA, United States
[e] Sandia National Laboratories, Energy Nanomaterials Department, Livermore, CA, United States
[f] College of Life Science and Technology, Beijing University of Chemical Technology, Beijing, China

ARTICLE INFO

Article history:
Received 7 April 2014
Received in revised form
20 February 2015
Accepted 22 February 2015
Available online 12 March 2015

Keywords:
Agave bagasse
Ionic liquid pretreatment
Lignocellulosic biofuels
Calcium oxalate
Characterization

ABSTRACT

Previous studies of agave bagasse (AGB-byproduct of tequila industry) presented unidentified crystalline peaks that are not typical from common biofuel feedstocks (e.g. sugarcane bagasse, switchgrass or corn stover) making it an important issue to be addressed for future biorefinery applications. Ionic liquid (IL) pretreatment of AGB was performed using 1-ethyl-3-methylimidazolium acetate ($[C_2mim][OAc]$) at 120, 140 and 160 °C for 3 h and a mass fraction of 3% in order to identify these peaks. Pretreated samples were analyzed by powder X-ray diffraction (XRD), Fourier transform infrared (FT-IR) spectroscopy, field emission scanning electronic microscopy (FE-SEM), thermal analysis (TGA-DSC) and wet chemistry methods. Previous unidentified XRD peaks on AGB at $2\theta = 15°$, 24.5° and 30.5°, were found to correspond to calcium oxalate (CaC_2O_4) in a monohydrated form. IL pretreatment with $[C_2mim][OAc]$ was observed to remove CaC_2O_4 and decrease cellulose crystallinity. At 140 °C, IL pretreatment significantly enhances enzymatic kinetics and leads to ~8 times increase in sugar yield (6.66 kg m^{-3}) when compared to the untreated samples (960 g m^{-3}). These results indicate that IL pretreatment can effectively process lignocellulosic biomass with high levels of CaC_2O_4.

1. Introduction

Various physical and chemical pretreatment methods, including steam explosion, ammonium fiber expansion, dilute acid, lime, and organic solvent pretreatments, have been demonstrated to be capable of mitigating the biomass recalcitrance for subsequent enzymatic saccharification in order to obtain biofuels or value added products [1–3]. Most of these pretreatment methods are not selective and often produce

* *Corresponding author*. Tel.: +52 311 211 8821.
E-mail address: japerez@uan.edu.mx (J.A. Perez-Pimienta).
http://dx.doi.org/10.1016/j.biombioe.2015.02.026

undesirable by products (e.g. acetic acid or furfural) that can inhibit the downstream fermentative conversion of the monosaccharides into ethanol and other products [4]. In the last decade, numerous studies have focused on the dissolution of lignocellulose in a variety of certain ionic liquids (ILs) exhibiting a high solubility which have developed into a novel pretreatment process [5]. Currently, the costs of ILs production is high because they are produced on a relatively small scale; with vigorous research in the search of cheap and efficient ILs and increasing demand for ILs, the cost will drop in the near future. Most of the ILs used for biomass pretreatment are stable up to 300 °C with processing conditions within 80–180 °C and are relatively benign with minimal environmental impact in water and air pollution [6]. Microcrystalline cellulose can be readily solubilized in some ILs and recovered by the addition of an anti-solvent, such as water or ethanol. Crystallinity of the regenerated cellulose is lower than cellulose in the untreated biomass and is more susceptible to enzymatic hydrolysis [7].

Ionic liquids based on imidazolium cations (e.g., 1-butyl-3-methyl imidazolium chloride ([C_4mim]Cl) and 1-ethyl-3-methylimidazolium acetate ([C_2mim][OAc]) have been reported to solubilize a significant portion of lignocellulose at concentrations ranging from 5 to more than 15% (depending on temperature, nature of the IL, particle size and time) and enhance the saccharification kinetics of the recovered product [8]. Several studies have demonstrated that certain ILs can effectively solubilize lignocellulosic biomass such as switchgrass, poplar, pine, and corn stover [2], suggesting their potential for use in pretreating lignocellulosic feedstocks.

It was recently shown by Perez-Pimienta et al. [9] that [C_2mim][OAc] can effectively pretreat agave bagasse (AGB) by removing a significant amount of lignin (~45%) and generates a product that is highly amorphous. In the same report it was observed unidentified crystalline peaks of high intensity of x-ray diffraction in untreated AGB at $2\theta = 15°$, 24.5° and 30.5°, that are not reported in diffraction patterns of other biofuel feedstocks such as switchgrass or corn stover. After IL pretreatment with [C_2mim][OAc] the intensity of these unidentified peaks decreased. Since AGB is considered as a potential biofuel feedstock, it is necessary to characterize and analyze all its components, which may cause interference during pretreatment and subsequent downstream processes (enzymatic saccharification and fermentation).

In the present study a comprehensive characterization of AGB was conducted in order to determine the origin and role of the previously observed and unidentified crystalline components. *Agave tequilana Weber* is a plant that is cultivated in Mexico and used as a raw material in the production of the alcoholic beverage tequila. The AGB is a residual fiber obtained from the process and represents 40% of the harvested plant, with an annual generation in Mexico of about 112 kt in a wet basis, and at the moment just a small fraction is being used for soil composting or as plywood, while the rest is accumulated in landfills [10,11]. In this work, we sought to understand the physicochemical changes of AGB as a function of IL pretreatment with [C_2mim][OAc], with an emphasis on the elucidation of the unidentified crystalline peaks present in the biomass which has been reported by a number of research papers [9,12–15].

The experiments were designed to use a similar approach as in our previous report [9] thereby replicate the biomass behavior and obtain similar unidentified peaks using powder X-ray diffraction. Characterization of untreated and IL pretreated AGB was performed to determine glucan, xylan and lignin contents. Delignification and other chemical changes were tracked by Fourier Transform Infrared (FTIR) spectroscopy. X-ray diffraction (XRD) was used to compare the crystallinity of AGB before and after [C_2mim][OAc] pretreatment. Thermal properties was evaluated using thermogravimetric analysis and differential scanning calorimetry (TGA-DSC). Supramolecular structures of AGB were examined by field emission scanning electron microscopy (FE-SEM). Finally, the saccharification kinetics and overall sugar yields were determined.

2. Experimental section

2.1. Materials and sample preparation

Agave bagasse (AGB) was donated by Destilería Rubio, a Tequila facility from Jalisco, Mexico. This facility only used plants aged 7–8 years and the plant without the leaves is cooked about 18 h in an autoclave. After the cooking, the plant is milled and compressed to separate the syrup from wet bagasse. AGB samples were collected, washed thoroughly with distilled water and dried in a convection oven. The biomass was milled with a Thomas-Wiley Mini Mill fitted with a 400 μm screen (Model 3383-L10 Arthur H. Thomas Co., Philadelphia, PA, USA) and stored at 4 °C in a sealed plastic bag. Cellic® CTec2 (Cellulase complex for degradation of cellulose) and HTec2 (Endoxylanase with high specificity toward soluble hemicellulose) were a gift from Novozymes (Davis, CA). Ionic liquid, 1-ethyl-3-methylimidazolium acetate ([C_2mim][OAc]), acetic acid, sodium acetate, sulfuric acid, 3,5-dinitrosalicylic acid (DNS), and sodium hydroxide were purchased from Sigma–Aldrich (St. Louis, MO). Acetyl bromide and hydroxylamine hydrochloride were purchased from Alfa Aesar (Ward Hill, MA).

2.2. Ionic liquid pretreatment

A mass fraction of 3% of an AGB/IL mixture was prepared by combining 300 mg of milled AGB with 9.7 g [C_2mim][OAc] (used as received) in a 50 cm^3 autoclave vial. The vials and the contents were heated in an oven (Thelco Laboratory oven, Precision Instruments, VA) at 120, 140 and 160 °C for 3 h [2]. All experiments were conducted in triplicates. After 3 h of incubation, 30 cm^3 of deionized water was slowly added into the biomass[C_2mim][OAc]$^{-1}$ slurry to recover the pretreated AGB. A precipitate formed immediately, and the samples were centrifuged at 10,000 *g* for 10 min. The supernatant containing IL was removed, and the precipitate was washed five times with additions of water in order to ensure that excess IL had been removed. The washing process was continued until the concentration of IL in the supernatant, as measured by Fourier transform infrared (FTIR) spectroscopy using a previously established technique [9], was less than 0.2%.

2.3. Chemical characterization

Sugars content of untreated and pretreated AGB samples were determined according to the standard analytical procedures of the National Renewable Energy Laboratory (NREL) using a two-step acid hydrolysis method [16,17] as described by Perez-Pimienta et al. [9]. The untreated and pretreated AGB samples were dried overnight at 80 °C to determine the moisture content and heated to 550 °C in a muffle furnace for 4 h to determine the ash content. The content of acid insoluble lignin was determined gravimetrically as the solid residue remaining after two-step hydrolysis. The liquid filtrates were used to determine the content of acid soluble lignin. Samples were diluted as appropriate, and their ultra-violet absorbance was recorded in an Agilent 8453 UV–Vis spectrophotometer. The lignin content was determined with the absorbance at 280 nm and calculated using an averaged extinction coefficient of 1775 $m^{-3}kg^{-1}\,m^{-1}$ [18]. Total concentration of lignin in the samples was calculated as the sum of the concentrations of acid-soluble lignin, and acid-insoluble lignin. All acid hydrolyzes were run in triplicate.

2.4. Crystallinity measurement

XRD patterns of untreated and pretreated AGB were collected with a PANalytical Empyrean X-ray diffractometer equipped with a PIXcel^{3D} detector and operated at 40 kV and 40 kA using Cu$K\alpha$ radiation. Samples from three replicates were mixed for XRD analysis. AGB samples were cast with double-sided tape on microscope slides. A reflection-transmission spinner was used as a sample holder and the spinning rate was 0.067 Hz. Patterns were collected in the 2θ range of 5–65°, the step size was 0.026°, and the exposure time was 300 s. The crystallinity index (CrI) was determined by curve fitting of the diffraction patterns using the software package HighScore Plus®.

2.5. Attenuated total reflectance (ATR)–FTIR spectroscopy

ATR–FTIR was conducted using a Bruker Optics Vertex system with built-in diamond-germanium ATR single reflection crystal. Untreated and pretreated AGB samples were pressed uniformly against the diamond surface using a spring-loaded anvil. Sample spectra were obtained in triplicates using an average of 128 scans over the range between 850 cm^{-1} and 2000 cm^{-1} with a spectral resolution of 2 cm^{-1}. Air, water and IL solution were used as background for untreated and pretreated biomass samples, respectively. Baseline correction was conducted using the rubber band method following the spectrum minima [8].

2.6. Analysis of morphology

The morphology and localized chemical information of untreated and pretreated AGB solids were analyzed using a field emission scanning electron microscope (FE-SEM) by a JEOL JSM-7600F equipment. Prior to acquiring images, the samples were mounted with double-sided carbon taped on precut brass sample stubs and coated with approximately 20 nm of gold using a sputtering system in order to avoid static change and kept in a desiccator until analysis. The representative images were acquired with a 7.5 kV accelerating voltage.

2.7. DSC and TGA analysis

A differential scanning calorimeter (DSC Q100) from TA Instruments was used with a N_2 atmosphere (50 $cm^3\,min^{-1}$) in the range of 25–256 °C, using a 10 $Kmin^{-1}$ ramp. DSC curves were obtained using 3.3 mg. The TGA curves were obtained using around 3.8 mg of AGB as initial sample mass. The bagasse was tested in a TGA SDT Q600 from TA Instruments, with temperature range of 25–800 °C and heating rate of 10K min^{-1} in N_2 atmosphere.

2.8. Enzymatic saccharification

Enzymatic saccharification using commercially available Cellic® CTec2 and HTec2 enzyme mixtures of untreated and pretreated AGB samples was conducted at 55 °C and 2.5 Hz in 9.6 kgm^{-3} citrate buffer (pH of 4.8). The untreated AGB were run concurrently with the samples to eliminate potential differences in temperature history or enzyme loading. The enzyme concentrations of CTec2 and HTec2 were set at 20 g protein per kg glucan and 2 g protein per kg xylan, respectively. Enzyme concentration for CTec2 and HTec2 were 188 and 24.6 kg protein m^{-3}, respectively. Enzyme activities for CTec2 and HTec2 were 320 $FPUcm^{-3}$ and 1300 xylanase $IUcm^{-3}$, respectively. All assays were performed in triplicate. Error bars show the standard deviation of triplicate measurements.

2.9. 3,5-Dinitrosalicylic acid (DNS) assay

Saccharification reactions were monitored by taking 50 mm^{-3} of the saccharification supernatant at specific time intervals (0, 0.5, 1, 3, 6, 24, 48 and 72 h). The collected samples were centrifuged at 10,000 *g* for 5 min, and reducing sugars were measured using the DNS assay on a DTX 880 Multimode Detector (Beckman Coulter, CA) [19]. Using glucose solutions in water as calibration standards. The initial rate of enzymatic saccharification was calculated based on the sugar released during the first 30 min of hydrolysis [20]. All assays were performed in triplicate.

3. Results and discussion

3.1. Compositional analysis

Previous studies have found that [C_2mim][OAc] is an effective solvent to solubilize the plant cell wall at relatively mild temperatures [21]. Subsequent cellulose precipitation and regeneration via addition of water as an anti-solvent leads to a fraction of lignin remaining dissolved in the mixture of IL and water [8]. As shown in Table 1, the chemical composition of untreated AGB (lignin-19.9%, xylan-19.8% and glucan-45.6%) is consistent with literature data [11]. After pretreatment with [C_2mim][OAc], the samples were enriched in carbohydrates (xylan + glucan) and reduced in lignin, which facilitated subsequent enzymatic hydrolysis. The recovered samples

Table 1 – Polymer and ash mass fractions (%) of untreated and IL treated AGB.

Agave bagasse	Glucan	Xylan	Arabinan	Galactan	Total lignin[a]	Acid-soluble lignin	Acid-insoluble lignin	Ashes	Moisture content
Untreated	45.6 ± 1.6	19.8 ± 0.7	4.3 ± 0.0	0.8 ± 0.7	19.9 ± 0.2	3.9 ± 0.1	16.0 ± 0.1	4.3 ± 0.1	7.4 ± 0.1
120 °C	52.6 ± 1.5	20.5 ± 1.4	0.1 ± 0.0	0.3 ± 0.1	16.7 ± 0.5	3.4 ± 0.4	13.3 ± 0.1	3.7 ± 0.1	1.4 ± 0.3
140 °C	46.9 ± 1.6	25.6 ± 0.8	0.1 ± 0.0	0.1 ± 0.1	15.2 ± 0.6	3.2 ± 0.2	12.0 ± 0.4	3.8 ± 0.2	2.1 ± 0.1
160 °C	66.4 ± 1.5	21.3 ± 1.7	0.1 ± 0.0	0.1 ± 0.1	12.8 ± 0.6	2.6 ± 0.3	10.2 ± 0.3	3.6 ± 0.1	1.4 ± 0.1

[a] Total lignin = Acid soluble lignin + Acid insoluble lignin.

after being treated at 120 and 160 °C for 3 h had higher glucan content when compared to untreated biomass (52.6 and 66.4% vs. 46.9%). The xylan content remained roughly constant (Supplementary data, Fig. I). It was, however, noted that the glucan content of the sample IL-140 °C was close to that of untreated AGB while the xylan content increased from 19.8 to 25.6%. It appears that the xylan is largely preserved while the cellulose suffered some losses after the biomass sample was pretreated at 140 °C. This contrasts with those of 120 and 160 °C while the cellulose was mostly preserved and xylan suffered some losses. We also noticed that based on TGA data, sample IL-140 °C became easier to thermally decompose, which suggests that at this temperature the IL pretreatment may have depolymerized both cellulose and xylan, but it is not clear why this would happen at 140 °C. For these reasons, we are planning further studies on the correlation of temperature, IL content and crystalline material content reported on the X-ray diffraction section. During IL pretreatment, total delignification was determined to be 16.1% at 120 °C, 21.6% at 140 °C and 35.7% at 160 °C. Currently, there are not many reports regarding the effectiveness of delignification from AGB. However, literature results for other agricultural residues suggest that it depends on biomass type and pretreatment conditions. daSilva et al. [22] reported a delignification up to 57.8% of wheat straw after pretreatment at 140 °C for 6 h. A recent study investigated the [C2mim][OAc] dissolution of sugarcane bagasse using a mass fraction of 5% at 120 °C for 0.5 h, and they achieved a lignin reduction of 32.1% [23]. Li et al. [2] hypothesized that the differences during IL pretreatment in the reported delignification efficiencies were likely due to the following reasons: the interactions of specific ionic liquids in pretreatment had an effect within the biomass which was dependent on the cation, anion, temperature, and time used in the process, and the extent and degree of biomass recalcitrance varies as a function of the biomass itself and was influenced by inherent variations in terms of age, harvest method, extent of drying, and storage conditions.

3.2. *X-ray diffraction*

The features of recovered AGB after IL pretreatment were examined using powder XRD and compared to the untreated sample. The measured XRD patterns are presented in Fig. 1A noticeable effect of IL pretreatment is the loss of sharp crystalline peaks at 2θ = 15°, 24.5° and 30.5° as a function of temperature. These peaks were previously reported, and were hypothesized that those signals were produced by an impregnated substance on the AGB during the fermentation process or byproducts confinement [9,12–15]. Those peaks are identified to be from calcium oxalate (CaC_2O_4) in a monohydrated form, this material is also known as whewellite. Fig. 2 shows the XRD patterns of untreated AGB and the calculated pattern for calcium oxalate monohydrate, generated from the published crystal structure by Deganello [24]. Crystalline features of the untreated AGB sample are in good agreement with the expected diffraction peaks for $CaC_2O_4{\cdot}H_2O$. The main peaks at 2θ = 15°, 24.5° and 30.5° correspond to the (10-1), (020) and (20-2) lattice planes in monoclinic $CaC_2O_4{\cdot}H_2O$, *I2* m^{-1}space group (Supplementary data, Fig. II) [24]. It also agrees well with other reports of CaC_2O_4 in plants, such as the report by Hartl et al. [25] The presence of calcium oxalate in biomass is well documented, with more than 215 plant families known to accumulate crystals within their tissues, including many crop plants that can accumulate calcium oxalate in the range of 3–80% of their dry weight, however, it is not present in this magnitude in any currently employed biofuel feedstock like corn stover or switchgrass [26]. The crystals have a variety of important functions, including tissue calcium regulation, plant protection and detoxification of heavy metals [27]. Besides, CaC_2O_4 traces can be found as calcite ($CaCO_3$) in the ash of untreated AGB (data not shown). It is noted that many Crassulacean acid metabolism (CAM) plants, which include cactus and agaves, have higher levels of calcium oxalate compared to other biofuel feedstocks [27].As can be observed from the XRD patterns, the IL pretreatment is efficient in removing most of the calcium oxalate phases. Moreover, calcium oxalate reacts exothermically with strong oxidants such as hydrogen

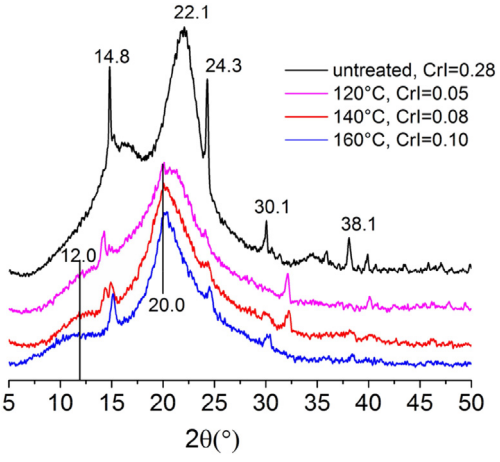

Fig. 1 – XRD spectrum of untreated and IL pretreated AGB.

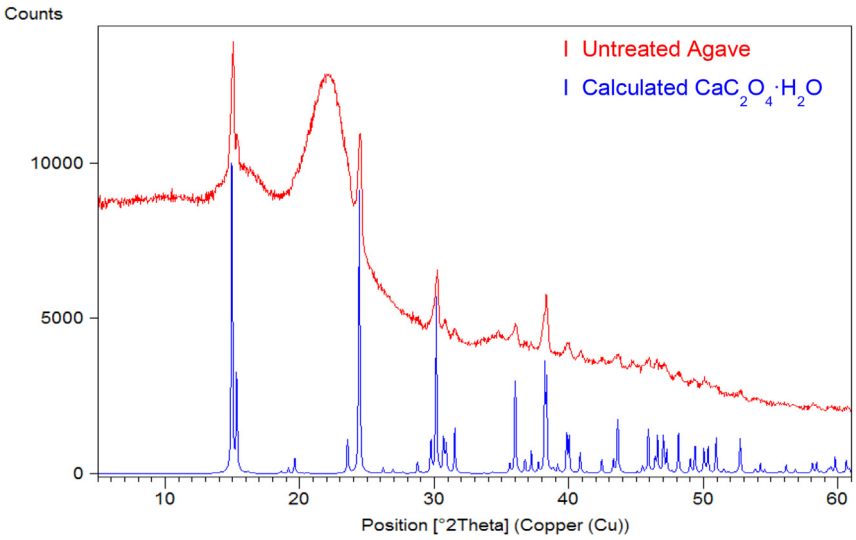

Fig. 2 – XRD spectrum of untreated AGB and calculated calcium oxalate monohydrate. The calculated $CaC_2O_4{\cdot}H_2O$ pattern was generated by Mercury™ (version 3.1) from published Crystallographic Information File.

peroxide or ozone but it does not react with biological agents [28]. It should be noted that further studies are needed to determine the effect of calcium oxalate in biomass pretreatments (especially oxidant ones) in terms of process efficiency and subsequent enzymatic saccharification.

XRD measurements provide one of the best options to estimate the impact of pretreatment on biomass crystallinity, which is believed to significantly affect enzymatic saccharification of glucan [29]. XRD is a robust methodology to determine the cellulose crystallinity index (CrI) and identify cellulose polymorphs. The CrI of the cellulose I lattice was estimated by separation of amorphous and crystalline contributions to the diffraction spectrum. The sample CrI of untreated AGB, defined as mass fraction of crystalline cellulose over whole biomass samples, is estimated to be 0.28. The cellulose CrI, obtained after normalizing to its cellulose content, equals to 0.61, which suggest that 61% of the cellulose is crystalline. After [C_2mim][OAc] pretreatment at 120 °C, the main peak at around 22.1° shifted to lower angle and became broader. Meanwhile, the broad peak at around 16.0°, which is a composite peak, dropped its intensity and became a weak shoulder peak. This effect has been reported before and is consistent with severely distortion of cellulose I lattice [30] and a decrease in crystallinity (sample CrI of ~5%). With increasing pretreatment temperature, a cellulose II structure evolved with the characteristic peaks at around 12.0° and 20.0°, which indicates partial dissolution of AGB samples. However the CrI of cellulose II is relatively low in these pretreated samples with the sample CrI of less than 10% and the cellulose CrI of less than 20%. Therefore, these IL pretreated samples are mainly amorphous.

3.3. *ATR-FTIR analysis*

Chemical fingerprinting of IL-pretreated and untreated AGB was characterized by ATR–FTIR, using a normalized spectra at a band position between 850 cm^{-1} and 2000 cm^{-1} (Supplementary data, Fig. III). For ATR–FTIR data, seven bands are used to monitor the chemical changes of lignin and carbohydrates, as well as the amorphous to crystalline cellulose ratio and two bands for changes in calcium oxalate intensity. The main antisymmetric carbonyl stretching band specific to the oxalate family occurs at 1618 cm^{-1} for $CaC_2O_4{\cdot}H_2O$ and the secondary carbonyl stretching band, the metal-carboxylate stretch, is located at 1317 cm^{-1}. Those two bands are observed to decrease with IL pretreatment in agreement with the peak reduction on XRD [31]. A decrease in the reduction in the 1745 cm^{-1} intensity associated with carbonyl C=O stretching occurs in the pretreated samples, this indicates cleavage of lignin side chains increasing slightly only at sample IL-160 °C. When compared to the untreated spectrum, the bands at 1510 cm^{-1} (aromatic skeletal from lignin) and 1375 cm^{-1} (C–H deformation in cellulose & hemicellulose) increase for IL-pretreated samples. However, usually the bands at 1510 cm^{-1} decreases after IL pretreatment [21], which reflects the degree of delignification. In this work, the lignin bands are affected by the broad and intense CaC_2O_4 peaks. Furthermore, a significant increase at 1056 cm^{-1} band (C–O stretch in cellulose & hemicellulose) is observed for all IL-pretreated sample, and a minor decrease in the band intensity at 1235 cm^{-1} (C–O stretching in lignin & hemicellulose) was observed for samples IL-120 °C and IL-140 °C, increasing its intensity only on sample IL-160 °C. This is likely due to the cleavage of ester linkages in lignin and hemicelluloses after pretreatment at 160 °C. In addition to that, the crystalline to amorphous cellulose ratio peaks of 1098 $cm^{-1}$and 900 cm^{-1} is decreasing as a function of the IL pretreatment temperature, which is consistent with the XRD pattern, indicating the decrease of cellulose crystallinity [2]. In comparison, an increase in the band intensity at 900 cm^{-1} (anti-symmetric out-of-plane ring stretch of amorphous cellulose) is observed in the spectra of IL-pretreated samples, which reflects the relative increase in cellulose content as a result of partial removal of both lignin and hemicellulose.

3.4. *Thermogravimetric and differential scanning calorimetry analysis*

Fig. 3 shows the differential TG plots rather than standard weight loss plots of untreated and IL pretreated AGB; that is, the function plotted is rate of weight loss (percent per degree centigrade) as function of temperature. All samples show three decomposition stages and some initial weight loss up to 125 °C (related to water loss associated with moisture present). The degradation onset temperature (T_s) is observed to decrease for IL treated samples as compared to the untreated AGB, shown in Table 2. A similar trend is also observed for thermal decomposition temperature (T_d) stage, in both cases the lowest value corresponds to IL-pretreated sample at 140 °C. These results indicate IL pretreatment reduced the activation energy that is needed to decompose woody biomass by deconstructing the tight plant cell wall structures. The temperature region between 220 and 300 °C is mainly attributed to thermal depolymerization of hemicelluloses, while lignin decomposition extends to the whole temperature range, from 200 °C until 700 °C, due to different activities of the chemical bonds present on its structure and the degradation of cellulose taken place between 275 and 400 °C [32]. The final decomposition of all samples was completed between 600 and 680 °C, attributed to secondary reactions of carbon-containing residues, which Fisher et al. [33] have shown that, at temperatures above 400 °C, a weight loss due to thermolysis of carbon containing residues does take place. When the T_s and T_d of the untreated AGB are compared to the IL-pretreated samples, a reduction is obtained corresponding to: sample IL-120 °C (2.4 and 1.6%), sample IL-140 °C (9.1 and 7.7%) and sample IL-160 °C (5.5 and 5.6%) for T_s and T_d, respectively. The decrease of both T_s and T_d is expected to occur due to the effect of IL pretreatment and associated lignin removal. Yang et al. [34] reported the pyrolysis characteristics of pure hemicellulose, cellulose and lignin at a heating rate of 10 $Kmin^{-1}$ in terms of maximum weight loss. They found that the decomposition temperature of hemicellulose and cellulose were 268 °C and 355 °C, respectively. Lignin was the most difficult to decompose, which happened slowly under the whole temperature range from ambient to 900 °C. Couhert et al. [35] stated that decomposition of pure components differs from real biomass because the pyrolysis reactions are less hindered by interaction with other components. Therefore, we hypothesize that the IL treated samples are thermally more stable in terms of decomposition temperatures after pretreatment that leads to a downshift in degradation temperatures, making them suitable for subsequent higher yields in enzymatic saccharification.

Table 2 – Onset T_s and decomposition T_d temperatures for untreated and IL pretreated AGB.

Property	Pretreatment			
	Untreated	IL-120 °C	IL-140 °C	IL-160 °C
T_s, °C	253	247	230	239
T_d, °C	376	370	347	355

Fig. 4 illustrates the DSC curves of untreated AGB and IL pretreated AGB (120, 140 and 160 °C) with two endothermic peaks observed. Vaporization temperatures and energy of AGB were estimated for untreated (94 °C – 25.2 J g^{-1}), sample IL-120 °C (77 °C – 26.42 J g^{-1}), sample IL-140 °C (90 °C – 12.7 J g^{-1}), and sample IL-160 °C (77 °C – 22.4 J g^{-1}). In addition, a slight curve corresponding to free water that evaporates before subsequent degradation stages can be observed in untreated AGB (154 °C – 0.6 J g^{-1}), sample IL-120 °C (150 °C–4.1 J g^{-1}), sample IL-140 °C (157 °C–5.8 J g^{-1}), and sample IL-160 °C (130 °C–1.5 J g^{-1}) samples. The IL-pretreated samples exhibit higher calorific values than the untreated AGB [35]. A recent report by Satyanarayana et al. [12] presented DSC curves for untreated AGB with one endothermic peak corresponding to dehydration at 89.2 °C and 328.1 J g^{-1}, which were higher than the energy values of 25.2 J g^{-1} at 94 °C

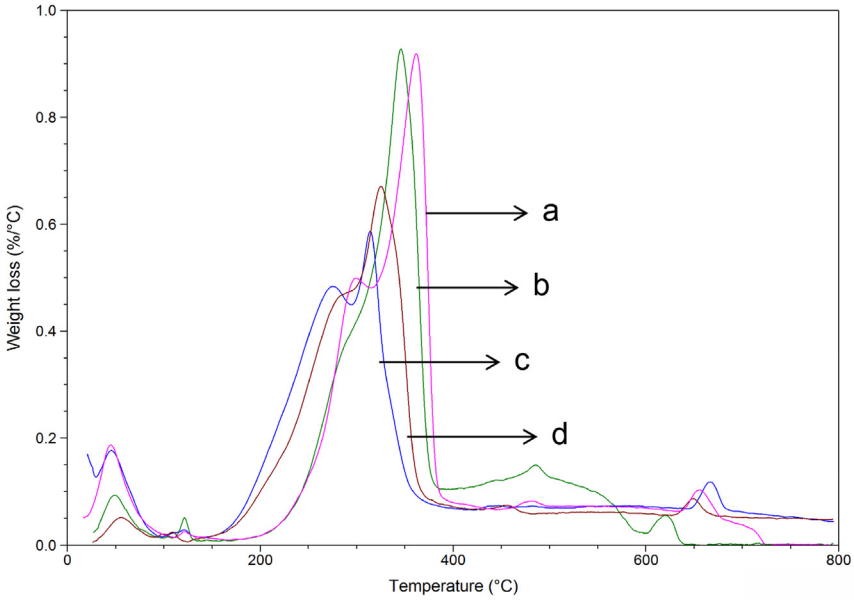

Fig. 3 – Differential TGA plot is shown for: a) untreated AGB and IL pretreatment at b) 120 °C, c) 140 °C and d) 160 °C.

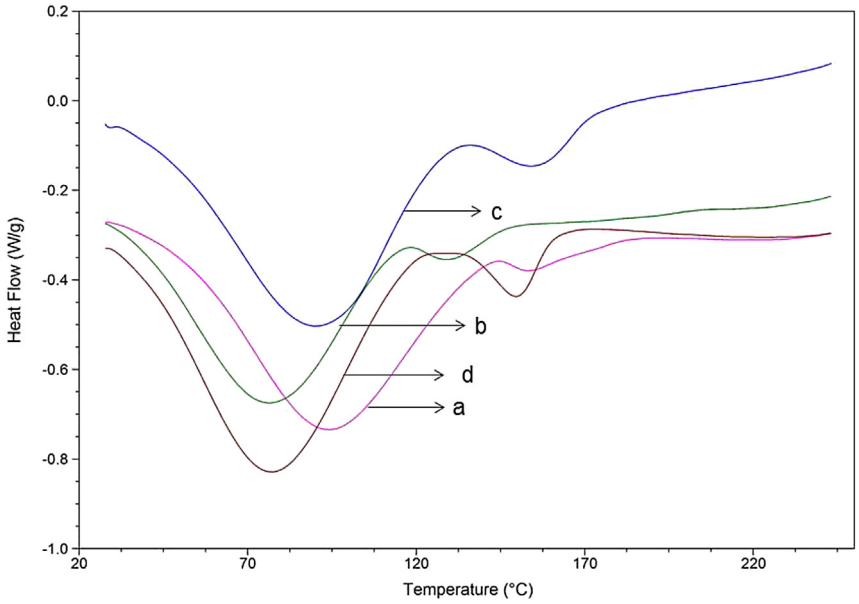

Fig. 4 – DSC results for: a) untreated AGB, IL pretreated at b) 120 °C, c) 140 °C and d) 160 °C.

in this study. These differences could be attributed to chemical composition and water content. It should be noted that this is not observed in a particular path or incidence of CaC_2O_4 in neither TGA nor DSC [36]. Finally, TGA-DSC analyses show that thermal degradation depends mainly on cellulose structure and biomass composition with higher calorific values found in the IL-pretreated samples.

3.5. *Field emission scanning electron microscope*

The FE-SEM images of untreated and IL pretreated AGB were taken at 5,000x and 10,000x magnification (Supplementary data, Figs. IV and V). The results show presence of recognizable but dispersed crystals of calcium oxalate in the untreated samples and more organized structures in the pretreated samples. IL pretreatment significantly alters the fibrillar structure and there are pores observed over several length scales. These results are consistent with the observations that faster hydrolysis rates and higher glucan yields are obtained for IL treated biomass. The presence of calcium oxalate crystals in considerable quantities are found in untreated AGB mainly in the form of styloid crystals dispersed along the surface [37]. Increasing the temperature of IL pretreatment induce to different forms of CaC_2O_4, such as crystals with dominating bypiramid prism in the 120 °C IL treated samples, this form can be found present in a cactus species (*Brachycereusnesioticus*) or in precipitates of CaC_2O_4 [37,38]. At the sample IL-140 °C CaC_2O_4 is confined into defined areas as spherical crystals and finally in the sample IL-160 °C the concentration of CaC_2O_4 was reduced and it cannot be found specific crystals, which is consistent with the XRD results of the lower quantity of CaC_2O_4.

3.6. *Enzymatic saccharification*

Enzymatic hydrolysis of both untreated and IL-pretreated AGB was carried out to compare their initial kinetics and cellulose digestibility. Cellulase cocktails derived from filamentous fungi are incompatible with ILs such as [C2mim][OAc]; therefore a watching step is necessary to remove residual IL from biomass prior to addition of enzymes [39]. Developing IL-tolerant enzymes and microorganisms to conduct enzyme hydrolysis and microbial fermentation in one bioreactor, or using aqueous IL solutions (20–50% IL) to pretreat biomass and potentially reduce the amount of washing required prior to enzymatic saccharification are some of the current options to make the IL pretreatment more efficient [40]. Fig. 5 shows total reducing sugar production for untreated and IL pretreated AGB with a mass fraction of 3%. When compared with untreated samples, the IL pretreated AGB exhibited significantly faster cellulose to sugar conversion. Additionally, the initial rates of hydrolysis and percentage of lignin removed as function of IL pretreatment temperature are shown in

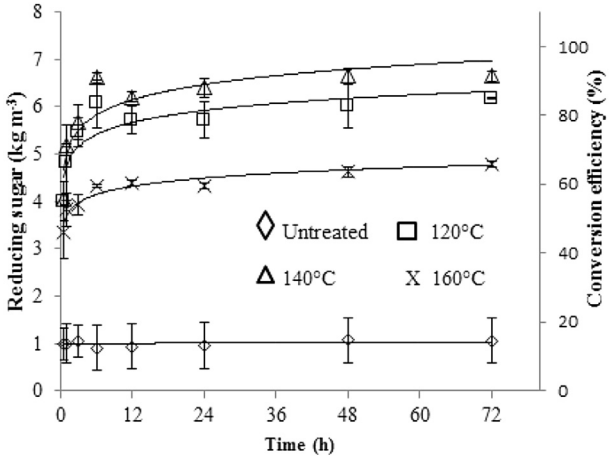

Fig. 5 – Enzymatic hydrolysis of untreated and IL pretreated AGB. Error bars show the standard deviation of triplicate measurements.

Supplementary data as Fig. VI. The amount of reducing sugars released during 24 h increased from 960 g m^{-3} to 5.72 kg m^{-3} from sample IL-120 °C, 5.39 kg m^{-3} from sample IL-140 °C and 4.33 kg m^{-3} from sample IL-160 °C, respectively. The initial hydrolysis rates were observed to be 0.133 kg $m^{-3}min^{-1}$at 120 °C, 0.135 kg $m^{-3}min^{-1}$at 140 °C and 0.112 kg m^{-3} min^{-1} at 160 °C. The maximum yields occurred for the sample pretreated at 140 °C (48 h hydrolysis - 6.66 kg m^{-3}) which can be correlated to its low T_s (230 °C) and T_d (347 °C). Furthermore, when compared to the untreated AGB, the sample IL-140 °C achieved an increase of ~8 times in its sugar yield. However, even with a higher level of delignification, sample IL-160 °C exhibited a lower sugar yield. Interestingly, sample IL-160 °C has a higher Ts (239 °C) and Td (355 °C) than those of sample IL-140 °C. It has been shown in the literature that decrystallization and delignification in general favor enzymatic hydrolysis, yet the degree of their impacts on the enzymatic hydrolysis varies with the type of biomass.

Due to the complex plant cell wall structures and their interactions with ILs at high temperatures, a clear understanding of the mechanism of IL pretreatment is still lacking, which was the reason we and also many other carried out investigations in this field. Several mechanisms can be related to an increase in yields of reducing sugar in enzymatic hydrolysis after IL pretreatment such as: an increased accessible surface area and porosity facilities subsequent saccharification, disrupting hydrogen bonds in native crystalline cellulose I resulted in a decreased cellulose crystallinity, delignification and depolymerization of hemicelluloses by disrupting the cross-linked matrix of lignin and hemicelluloses in which cellulose microfibrils are embedded.

Having said that, after IL pretreatment, many chemical and physical changes are coupled together which present their overall effect as improved enzymatic hydrolysis. The delignification alone sometimes may not stand out as other factors may overwhelm. For example, in a recent study by DeMartini et al. [41], the delignification played a less important role than hemicellulose removal in improving enzymatic hydrolysis in switchgrass.

4. Conclusions

The chemical and structural changes of AGB as a function of IL pretreatment using [C_2mim][OAc] were investigated. Previously unidentified peaks in the XRD patterns at $2\theta = 15.0°$, 24.5° and 30.5°, were found to correspond to calcium oxalate (CaC_2O_4) in a monohydrated form. High sugar yields were obtained for all AGB samples treated with [C2mim][OAc], with a maximum yield of 6.66 kg m^{-3} from the sample IL-140 °C, which is about 8 times higher when compare to the untreated AGB. The content of calcium oxalate is observed to be reduced in the recovered product as a function of IL pretreatment temperature. These results indicate that IL pretreatment is a promising pretreatment process for AGB in terms of efficiency, total process time, and high yields of sugar obtained from the recovered product when compared to the untreated samples. Finally, specific studies are needed to determine the effect of calcium oxalate in biomass pretreatments in terms of efficiency and subsequent enzymatic saccharification.

Acknowledgments

The authors thank Novozymes for the gift of the Cellic® CTec2 and HTec2 enzyme cocktails, and Damaris Cabrero Palomino for her assistance on TGA-DSC analysis. This work was part of the DOE Joint BioEnergy Institute (http://www.jbei.org) supported by the US Department of Energy, Office of Science, Office of Biological and Environmental Research, through Contract DE-AC02-05CH11231 between Lawrence Berkeley National Laboratory and the US Department of Energy. Gang Cheng acknowledges support by the joint funds of National Natural Science Foundation of China and Large Scale Scientific Facility of Chinese Academy of Science (U1432109).

Abbreviation used

[C_2mim][OAc]	1-ethyl-3-methylimidazolium acetate
AGB	agave bagasse
ATR–FTIR	Attenuated total reflectance – Fourier transform infrared spectroscopy
CrI	crystallinity index
DSC	differential scanning calorimetry
FE – SEM	field emission scanning electron microscope
IL	ionic liquid
T_d	thermal decomposition temperature
TGA	thermogravimetric analysis
T_s	degradation onset temperature
XRD	X-Ray diffraction
Sample IL-120 °C	sample pretreated at 120 °C
Sample IL-140 °C	sample pretreated at 140 °C
Sample IL-160 °C	sample pretreated at 160 °C

Appendix A. Supplementary data

Supplementary data related to this article can be found at http://dx.doi.org/10.1016/j.biombioe.2015.02.026.

REFERENCES

[1] Wang Y, Radosevich M, Hayes D, Labbé N. Compatible ionic liquid-cellulases system for hydrolysis of lignocellulosic biomass. Biotechnol Bioeng 2010;108(5):1042–8.
[2] Li C, Knierim B, Manisseri C, Arora R, Scheller HV, Auer M, et al. Comparison of dilute acid and ionic liquid pretreatment of switchgrass: biomass recalcitrance, delignification and enzymatic saccharification. Bioresour Technol 2010;101(13):4900–6.
[3] Mosier N, Wyman C, Dale B, Elander R, Lee YY, Holtzapple M, et al. Features of promising technologies for pretreatment of lignocellulosic biomass. Bioresour Technol 2005;96(6):673–86.
[4] Mosier N, Sarikaya A, Ladisch CM, Ladisch MR. Characterization of dicarboxylic acids for cellulose hydrolysis. Biotechnol Progr 2001;17(3):474–80.
[5] da Costa Lopes AM, João KG, Rubik DF, Bogel-Lukasik E, Duarte LC, Andreaus J, et al. Pre-treatment of lignocellulosic

biomass using ionic liquids: wheat straw fractionation. Bioresour Technol 2013;142(1):198–208.
[6] Guragain YN, Coninck JD, Husson F, Durand A, Rakshit SK. Comparison of some new pretreatment methods for second generation bioethanol production from wheat straw and water hyacinth. Bioresour Technol 2011;102(6):4416–24.
[7] Zhao H, Jonesa CL, Bakerb GA, Xia SQ, Olubajo O, Persona VN. Regenerating cellulose from ionic liquids for an accelerated enzymatic hydrolysis. J Biotechnol 2009;139(1):47–54.
[8] Singh S, Simmons BA, Vogel KP. Visualization of biomass solubilization and cellulose regeneration during ionic liquid pretreatment of switchgrass. Biotechnol Bioeng 2009;104(1):68–75.
[9] Perez-Pimienta JA, Lopez-Ortega MG, Varanasi P, Stavila V, Cheng G, Singh S, et al. Comparison of the impact of ionic liquid pretreatment on recalcitrance of agave bagasse and switchgrass. Bioresour Technol 2013;127(1):18–24.
[10] Saudedo-Luna J, Castro-Montoya AJ, Martinez-Pacheco MM, Sosa-Aguirre CR, Campos-Garcia J. Efficient chemical and enzymatic saccharification of the lignocellulosic residue from *Agave* tequilana bagasse to produce ethanol by *Pichia caribbica*. J Ind Microbiol Biotechnol 2011;38(6):725–32.
[11] Davis SC, Dohleman FG, Long SP. The global potential for Agave as a biofuel feedstock. GCB Bioenergy 2011;3(1):68–78.
[12] Satyanarayana KG, Flores-Sahagun THS, Dos Santos LP, Dos Santos J, Mazzaro I, Mikowski A. Characterization of blue agave bagasse fibers of Mexico. Compos. Part A Appl Sci 2013;45(1):153–61.
[13] Tronc E, Hernández-Escobar CA, Ibarra-Gómez R, Estrada-Monje A, Navarrete-Bolaños J, Zaragoza-Contreras EA. Blue agave fiber esterification for the reinforcement of thermoplastic composites. Carb Poly 2007;67(2):245–55.
[14] Velazquez-Jimenez LH, Pavlick A, Rangel-Mendez JR. Chemical characterization of raw and treated agave bagasse adsorbent of metal cations from water. Ind Crop Prod 2013;43(1):200–6.
[15] El Oudiani A, Chaabouni Y, Msahli S, Sakli F. Crystal transition from cellulose I to cellulose II in NaOH treated *Agave americana* L- fibre. Carb Poly 2011;86(3):1221–9.
[16] Sluiter A, Hames B, Ruiz R, Scarlata C, Sluiter J, Templeton D, et al. Determination of structural carbohydrates and lignin in biomass. Golden, Colorado:: National Renewable Energy Laboratory; 2011, Jul 08. Report No. TP-510–42618.
[17] Sluiter A, Hames B, Ruiz R, Scarlata C, Sluiter J, Templeton D. Determination of ash in biomass. Golden, Colorado: National Renewable Energy Laboratory; 2008. Jan, Report No. TP-510–42622.
[18] Fukushima RS, Hatfield RD. Comparison of the acetyl bromide spectrophotometric method with other analytical lignin methods for determining lignin concentration in forage samples. J Agric Food Chem 2004;52(12):3713–20.
[19] Miller GL. Use of dinitrosalicylic acid reagent for determination of reducing sugar. Anal Chem 1959;31(3):426–8.
[20] Dadi AP, Varanasi S, Schall CA. Enhancement of cellulose saccharification kinetics using an ionic liquid pretreatment step. Biotechnol Bioeng 2006;95:904–10.
[21] Li C, Cheng G, Balan V, Kent MS, Ong M, Chundawat SP, et al. Influence of physico-chemical changes on enzymatic digestibility of ionic liquid and AFEX pretreated corn stover. Bioresour Technol 2011;102(13):6928–36.
[22] da silva SPM, da Costa Lopes AM, Roseiro LB, Bogel-Lukasik R. Novel pre-treatment and fractionation method for lignocellulosic biomass using ionic liquid. RSC Adv 2013;3(1):16040–50.
[23] Qiu Z, Aita GM. Pretreatment of energy cane bagasse with recycled ionic liquid for enzymatic hydrolysis. Bioresour Technol 2013;129(1):532–7.
[24] Deganello S. The structure of whewellite $CaC_2O_4.H_2O$ at 328 K. Acta Cryst 1981;B37(4):826–9.
[25] Hartl WP, Klapper H, Barbier B, Ensikat HJ, Dronskowski R, Müller P, et al. Diversity of calcium oxalate crystals in Cactaceae. Can J Bot 2007;85(5):501–17.
[26] Nakata PA. Advances in our understanding of calcium oxalate crystal formation and function in plants. Plant Sci 2003;164(6):901–9.
[27] Monje PV, Baran EJ. Characterization of calcium oxalate biominerals in some (non-cactaceae) succulent plant species. Z Naturfosch C J Biosci 2010;65:429–32.
[28] Franceschi VR, Nakata PA. Calcium oxalate in plants: formation and function. Annu Rev Plant Biol 2005;56(7–8):41–71.
[29] Kumar R, Mago G, Balan V, Wyman CE. Physical and chemical characterizations of corn stover and poplar solids resulting from leading pretreatment technologies. Bioresour Technol 2009;100(17):3948–62.
[30] Cheng G, Varanasi P, Arora R, Stavila V, Simmons BA, Kent MS, et al. Impact of ionic liquid pretreatment conditions on cellulose crystalline structure using 1-ethyl-3-methylimidazolium acetate. J Phys Chem B 2012;116(33):10049–54.
[31] Ouyang J-M, Duan L, Tieke B. Effects of carboxylic acids on the growth of calcium oxalate nanoarticles in lecithin-water liposome systems. Langmuir 2003;19(21):8980–5.
[32] Deepa B, Abraham E, Cherian BM, Bismarck A, Blaker JJ, Pothan LA, et al. Structure, morphology and thermal characteristics of banana nano fibers obtained by steam explosion. Bioresour Technol 2011;102(2):1988–97.
[33] Fisher T, Hajaligol M, Waymack B, Kellogg D. Pyrolysis behavior and kinetics of biomass derived materials. J Anal Appl Pyrolysis 2002;62(2):331–49.
[34] Yang H, Yan R, Chen H, Lee DH, Zheng C. Characteristics of hemicellulose, cellulose and lignin pyrolysis. Fuel 2007;86(12):1781–8.
[35] Couhert C, Commandre JM, Salvador S. Is it possible to predict gas yields of any biomass after rapid pyrolysis at high temperature from its composition in cellulose, hemicellulose and lignin. Fuel 2009;88(3):408–17.
[36] Prychid CJ, Rudall PJ. Calcium oxalate crystals in monocotyledons: a review of their structure and systematics. Ann Bot 1999;84(6):725–39.
[37] Girija EK, Latha SC, Kalkura SN, Subramanian C, Ramasamy P. Crystallization and microhardness of calcium oxalate monohydrate. Mat Chem Phys 1998;52(3):253–7.
[38] Ulmgren P, Rådeström R. Solubility and mehcanism of calcium oxalate in D (chlorine dioxide stage) filtrates. J Pulp Pap Sci 2001;27(11):391–6.
[39] Gladden JM, Park JI, Bergmann J, Reyes-Ortiz V, D'haeseleer P, Quirino BF, et al. Discovery and characterization of ionic liquid-tolerant thermophilic cellulases from a switchgrass-adapted microbial community. Biotechnol Biofuels 2014;7(15):1–12.
[40] Li C, Tanjore D, He W, Wong J, Gardner JL, Sale KL, et al. Scale-up and evaluation of high solid ionic liquid pretreatment and enzymatic hydrolysis of switchgrass. Biotechnol Biofuels 2013;6(154):1–13.
[41] DeMartini JD, Pattahil S, Miller JS, Li H, Hahn MG, Wyman CE. Investigating plant cell wall components that affect biomass recalcitrance in poplar and switchgrass. Energy Environ Sci 2013;6(1):898–909.